Journal of ELECTRONIC MATERIALS, Vol. 50, No. 4, 2021
https://doi.org/10.1007/s11664-020-08356-8

ASIAN CONSORTIUM ACCMS–INTERNATIONAL CONFERENCE ICMG 2020

Structural Characterization and Photoluminescent Behavior of CO_3 Intercalated Zn-Fe Layered Double Hydroxide (LDH) and its Colloids

VIJAYALAXMI THITE[1] and SUSHAMA M. GIRIPUNJE[1,2]

1.—Department of Physics, Visvesvaraya National Institute of Technology, Nagpur, Maharashtra 440010, India. 2.—e-mail: sushamagiripunje9@gmail.com

Carbonate intercalated Zn-Fe layered double hydroxide (LDH) with Zn^{2+}/Fe^{3+} molar ratios 2, 3 and 4 were synthesized by coprecipitation in order to study the photoluminescent (PL) properties of their colloids with various wt.% of LDH in formamide. These synthesized LDHs were characterized by various techniques including x-ray diffraction analysis (XRD), Fourier-transform infrared spectroscopy (FTIR), field emission scanning electron mMicroscopy (FE-SEM), energy-dispersive x-ray spectroscopy (EDS), high-resolution transmission electron microscopy (HR-TEM), and photoluminescence spectroscopy (PL). The rhombohedral phase and crystallite size of Zn-Fe LDH were confirmed by XRD. Crystallite size plays an important role in the PL mechanism. HR-TEM showed hexagonal nanosheets with 5–6 nm average particle size. To investigate the PL mechanism of pristine LDH and their colloids, these prepared Zn-Fe LDHs were exfoliated in formamide by varying their Zn^{2+}/Fe^{3+} molar ratios (2,3, 4) and LDH concentration (0.2 wt.%, 0.4 wt.%, 0.6 wt.%, 0.8 wt.% of LDH). Results revealed that surface charge density and surface defects are the main reasons for PL generation in LDH colloids.

Key words: LDH (layered double hydroxide), photoluminescence, colloids, coprecipitation, exfoliation

INTRODUCTION

LDHs (layered double hydroxides) comprise a class of useful multi-functional materials that attracts much research. LDHs were first used mostly in the water purification field, but later on showed promising applications in catalysis, biotechnology, nanotechnology, and sensors.[1–7] The ability to incorporate various compositional metal ions to suit the required applications is the most advantageous feature of LDH materials. The use of various intercalating anions in LDH also gives a promising path for future research.

(Received March 6, 2020; accepted July 23, 2020; published online August 9, 2020)

The general formula of LDH is $\left[MII_{1-x}MIII_x \cdot (OH)_2\right]^{x+}\left[A^{n-}_{x/n} \cdot yH2O\right]^{x-}$, where M(II) and M(III) are divalent and trivalent metal cations (these can also be monovalent or higher valence cations such as Sn^{4+}, Zr^{4+}, Li^{+}, Ti^{4+}) and A^{n-} is an n-valent intercalating anion. LDHs have a layered structure that offers a range of variations in exchangeable anions, cations, and their molar ratios.[8] The use of low-toxic, biocompatible Fe^{3+}, Mg^{2+}, Al^{3+}, Zn^{2+} cations in the cationic sheets of LDH, for example, allows using these solids as carriers for bioactive species. LDHs have been used in fields of biomedicine,[9] environmental applications,[10] drug storage,[11] etc. A large number of investigations on the intercalation of bioactive species in LDH for amino acids and drugs have been carried out in many research papers and reviews.[12–20] These materials also provide choices

in their synthesis procedures according to the application.

Morphologies and various hierarchial architectures are based on sophisticated synthesis with careful optimization of reaction conditions. Hence the synthesis method defines the features of a developed LDH.[21] There are several routes of synthesis for LDHs; the most commonly used are coprecipitation, ion exchange route, and reconstruction route. Coprecipitation is most frequently used as the direct synthesis route of LDH. In the coprecipitation condensation of hexa-aqua metal complexes is followed by the formation of a brucite-like structure.[10] There are two modes of operation in the coprecipitation method used for the synthesis of LDHs: variable pH and constant pH. The latter is used the most because it provides the minimal formation of undesired metal hydroxide radicals.[22] Particle size, crystallinity, surface area, and pore diameter parameters depend on the synthesis procedure. These are directly related to the various applications of LDHs. The coprecipitation method at constant pH is in good agreement with these parameters as compared to the variable pH method.[23] One of the major benefits of coprecipitation is it can be applied to large scale production of LDHs.

Zn-Fe LDH has been synthesized by fixing the Zn/Fe ratio while varying the intercalated anions such as CO_3^{2-}, NO^{3-}, and Cl^{-}.[24] Carbonate is the most common charge-balancing anion.[25] Carbonate intercalated LDHs are more easily synthesized, but it is difficult to exchange the carbonate for other anions in neutral or slightly alkaline systems. This material shows its most crystalline phase at divalent and trivalent molar ratios.[26,27] Carbonate intercalated LDHs showed best photocatalytic activity under visible light irradiation due to their high surface area, larger pore volume, suitable band gap energy and high adsorption ability.[28,29] Intercalation of CO_3^{-} helps to improve photoluminescence intensity by improving the crystallinity and morphology of particles.[30] It also increases the aggregation of particles, which boosts photoluminescence intensity.[31]

The high affinity of carbonate anions for LDH layers opposes direct exfoliation or direct anion exchange, hence delamination of LDH is quite challenging. Exfoliation or delamination of LDHs in *N*,*N*-dimethylformamide–ethanol was described by Gordijo et al. [32] There are various applications of these exfoliated LDHs as composite films with anionic polymers,[33] highly oriented thin films,[34] nanocomposites with neutral synthetic organic polymers,[35–37] quantum dot composites [38] and building blocks for the preparation of hollow spheres.[39] LDH nanosheets can also be obtained through a reproducible path by exfoliating their nitrates in formamide.[40]

Exchange of the interlayer anions by intercalation or adsorption of the fluorescent ions on the surface layers of the LDHs is the conventional method to obtain their photoluminescent composites. The photoluminescence properties of colloids of LDH have rarely been studied. This study aims to shed light on the PL mechanisms in pristine Zn-Fe LDH and its colloid, and also on the effect on PL of Zn^{2+}/Fe^{3+} molar ratio and the concentration of LDHs in their colloids.

MATERIALS AND METHODS

Zinc nitrate hexahydrate ($Zn(NO_3)_2{\cdot}6H_2O$), ferric nitrate ($Fe(NO_3)_2{\cdot}9H_2O$), sodium hydroxide (NaOH), sodium carbonate (Na_2CO_3) and formamide (CH_3NO) of AR grade were purchased from Merck and used without further purification.

Synthesis of Zn-Fe LDH

Zn-Fe LDHs with different Zn^{2+}/Fe^{3+} ratios were synthesized by a simple & cost-effective coprecipitation method. A homogeneously stirred solution of NaOH and Na_2CO_3 was added dropwise to solution of $Zn(NO_3)_2{\cdot}6H_2O$ and $Fe(NO_3)_2{\cdot}9H_2O$ until pH reached 10; the solution appeared reddish-brown in color. The precipitate was washed with double distilled water and dried at 85°C for 24 h. The resultant product was crushed to a fine powder for further investigation. The same procedure was followed for all samples with Zn^{2+}/Fe^{3+} in 2:1, 3:1 and 4:1 proportions. These samples were labeled as ZF2, ZF3, and ZF4.

Synthesis of Zn-Fe LDH Colloids

Colloids of Zn-Fe LDHs were prepared by delaminating 0.2, 0.4, 0.6 and 0.8 wt.% of Zn-Fe LDH in 100 ml formamide. Exfoliation was achieved by stirring the mixture for 72 h in an airtight container at room temperature, resulting in translucent suspension. The exfoliation of LDH is illustrated in Fig. 1.

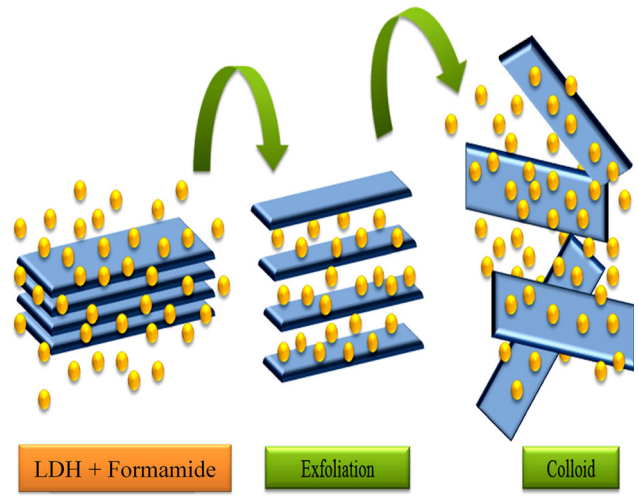

Fig. 1. Exfoliation of LDH in formamide.

CHARACTERIZATIONS

The XRD pattern of Zn-Fe LDH recorded by x-ray diffractometer with Cu Kα radiation (k = 0.154059 nm) at a scan rate of 2°/min was used to determine crystallite size. The diffraction pattern was recorded with a step size of 0.03. A Fourier transform infrared (FTIR) spectrum of the solid materials was obtained using a Shimadzu IR Prestige-21 FTIR spectrometer in the range 4000–400 cm^{-1}. The elemental composition of the prepared sample was studied by energy dispersive spectroscopy (EDS) on a JEOL microscope (JSM-7610F). Particle size determination and lattice fringe observation were performed by a high-resolution transmission electron microscope (HR-TEM, 300 kV). The photoluminescence of colloids was studied using an F-4600 FL spectrophotometer at 325 nm excitation wavelength.

RESULTS AND DISCUSSION

The XRD spectra of Zn-Fe-CO_3 LDHs prepared with Zn^{2+}/Fe^{3+} molar ratios 2, 3 and 4 (ZF2, ZF3 and ZF4) are shown in Fig. 2a. Typical peaks of the layered structure consist of symmetric and sharp peaks with high intensity at lower diffraction angles and asymmetric and broad peaks at a higher diffraction angle. These reflections correspond to LDH characteristics planes (003), (006), (015) and (012) at 11.98°, 23.63°, 38.89° & 46.28°, respectively.[41,42] The diffraction patterns indicate the crystalline structure of prepared LDHs. The extra peaks in the XRD spectra of ZF4 at 31.07, 68.06, 69.15°, corresponding to the (100), (112), (201) planes, reveal the presence of ZnO. This may be due to an increase in Zn content as compared to ZF2 and ZF3. The rhombohedral phase was confirmed and matched with JCPDS file 03-0486. Crystallite size was calculated by using Scherer's formula Eq. 1, and was found to be 11.37 nm for ZF4, 9.54 nm for ZF3, and for ZF2 it reduced to 8.86 nm. Also, when the molar ratio of Zn^{2+}/Fe^{3+} increased to 4:1, extra ZnO was formed, due to an increase in Zn^{2+}, whereas Fe^{3+} was constant for all the LDH samples. Scherer's formula is

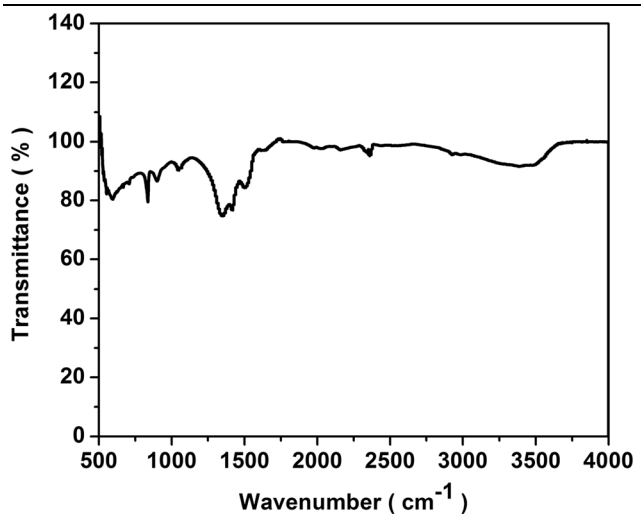

Fig. 3. FTIR spectra of Zn-Fe LDH.

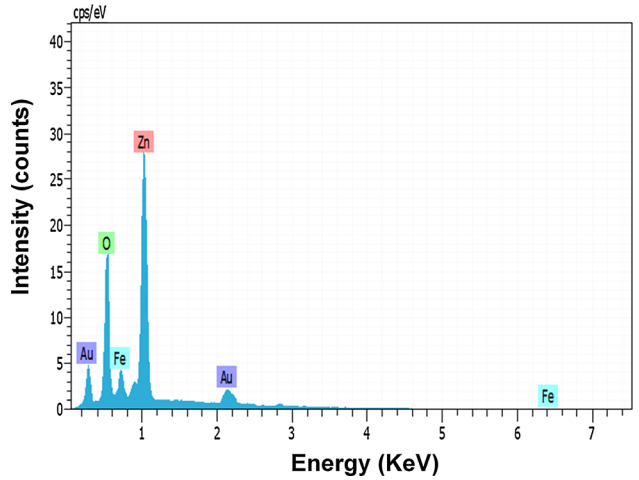

Fig. 4. EDS of Zn-Fe LDH.

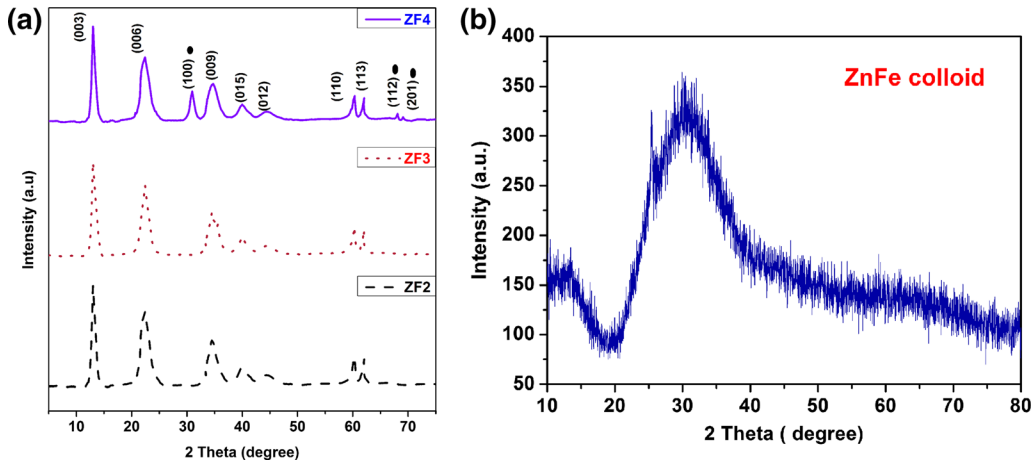

Fig. 2. (a) XRD profile of the Zn-Fe LDHs (b) XRD profile of Zn-Fe LDH colloid.

Table I. Elemental composition of Zn-Fe LDH

Element	Atomic %
Zn	28.79
Fe	4.89
O	17.81

$$D = k\lambda/\beta\cos\theta \quad (1)$$

where k is shape factor (0.9), λ is the x-ray wavelength used (Cu/Kα = 0.154 nm), β is the full width at half-maximum of the diffraction peak and θ is the angle of diffraction. The average lattice parameters were found to be a = b = 0.38 nm & c = 2.46 nm. A centrifuged gel-like product of colloid was collected to study using XRD. In XRD of Zn-Fe

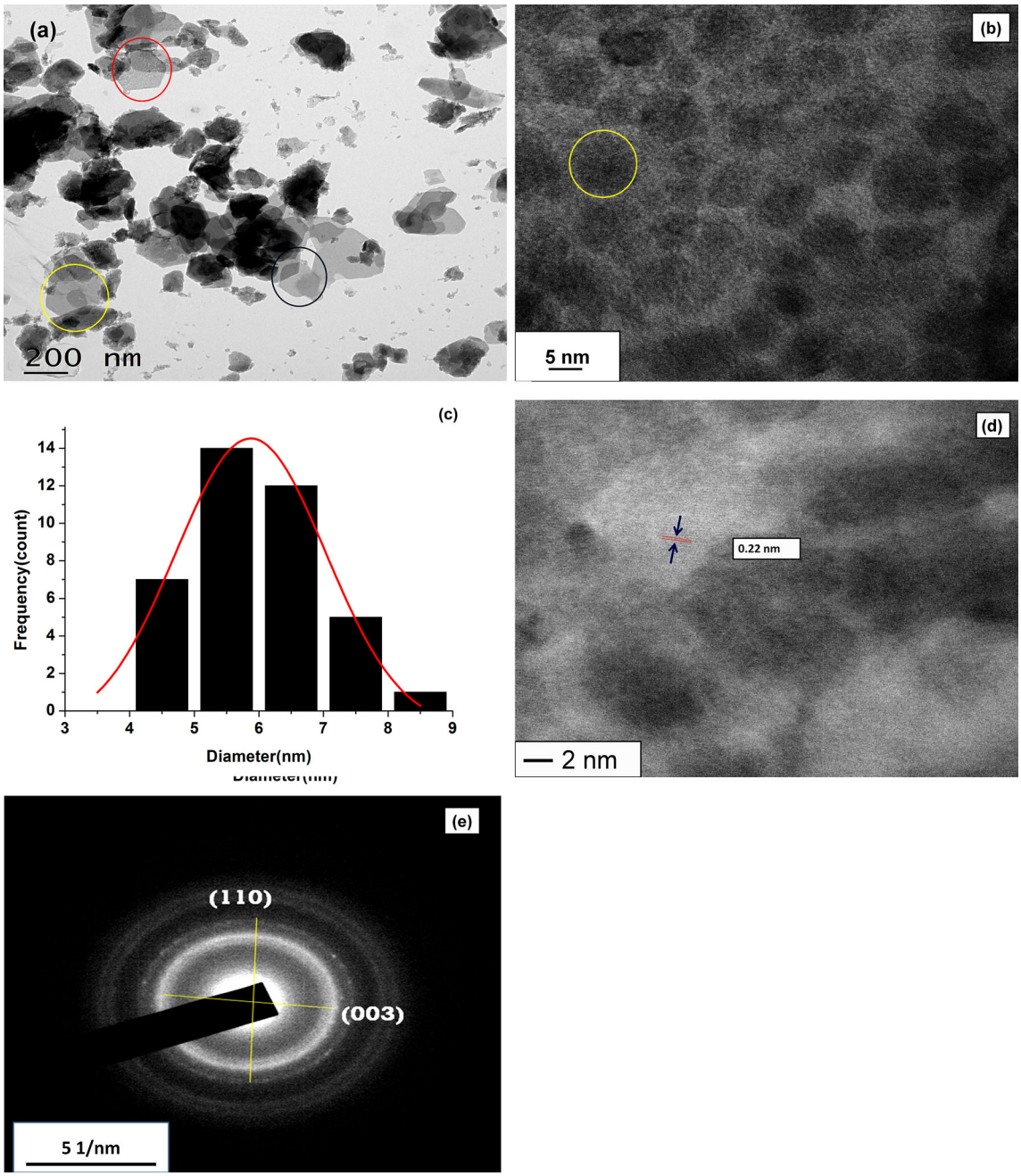

Fig. 5. (a), (b) HR-TEM images (c) average particle size distribution (d) lattice fringe spacing (e) SAED pattern of Zn-Fe LDH.

LDH colloids shown in Fig. 2b, the broad hump is due to formamide and the absence of any sharp peaks indicates that the LDH structure of Zn-Fe LDH was broken due to exfoliation.

The FT-IR spectrum of Zn-Fe LDH is shown in Fig. 3. The broad band between 3400 cm^{-1} & 3640 cm^{-1} arises due to the stretching of the OH bond of H_2O. A band at 1630 cm^{-1} belongs to the H_2O bending vibration of the interlayer water molecules. A sharp band at 1355 cm^{-1} corresponds to the carbonate ion stretching; the absorption band below 1000 cm^{-1} corresponds to M–O vibration modes of LDH.[43] To determine the elemental composition, energy-dispersive x-ray spectrum was carried out. EDS results shown in Fig. 4 provide atomic wt.% elemental composition, which reveals that Zn and Fe were unevenly present in synthesized LDH as listed in Table I.

The sizes and shapes of Zn-Fe LDH nanoparticles can be observed from the TEM images shown in Fig. 5a, b. Particle size calculated by using a particle size distribution histogram represented in Fig. 5c was found to be 5–6 nm. Lattice fringe spacing was measured at about 0.22 nm, representing the distance between two lattice planes, as shown in Fig. 5d. The SAED pattern shown in Fig. 5e represents diffraction rings containing continuous lattice fringes in different directions which are indexed to (003), (006), and (012) planes.

PHOTOLUMINESCENCE OF COLLOIDS OF ZN-FE LDH

Zn-Fe LDH colloids were prepared by exfoliating Zn-Fe LDH in formamide. The exfoliation process promotes the molecular interaction of LDH with the organic solvent formamide. This may be the effect of hydrogen bonding between formamide and LDH nanosheets.[44] These increased molecular interactions also increase surface defects, which facilitate electron–hole recombination.[45] In the case of pristine LDH, uniform exfoliation results in a high specific surface area, leading to increased surface defects which act as traps required for PL generation. Emission spectra of powder Zn-Fe LDH and colloid of Zn-Fe LDH excited at 325 nm are compared in Fig. 6, which represents the different shapes of emission peaks as the colloids contribute larger Stokes shifts than solids.[46] This points to a different PL mechanism in pristine LDH than in its colloid. Different shapes of emission spectra of powdered samples and suspension were also observed in the case of ZnO nanoparticles.[47–49]

The emission spectra of colloids of Zn-Fe LDH with varying Zn/Fe molar ratios excited at 325 nm are shown in Fig. 7, where colloids of ZF2, ZF3 and ZF4 are labeled as ZF2L, ZF3L and ZF4L. Due to compositional or lattice defects, an emission peak appears at 441 nm for all colloid samples. Photoluminescent intensity of Zn-Fe LDH colloid decreases with an increase in the Zn^{2+}/Fe^{3+} molar ratio. This

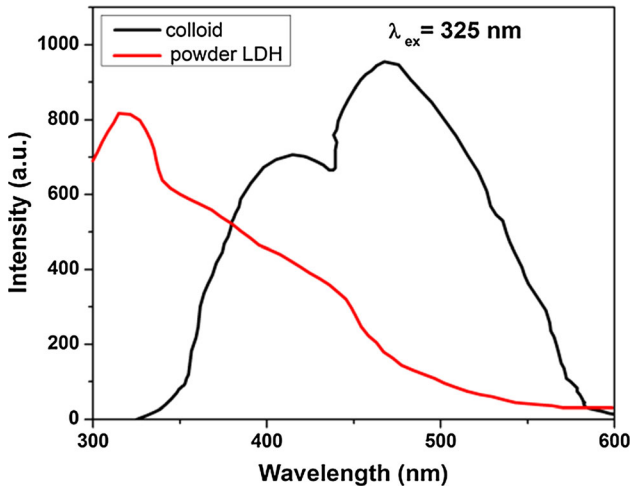

Fig. 6. PL EM spectra of solid Zn-Fe LDH and its Colloid.

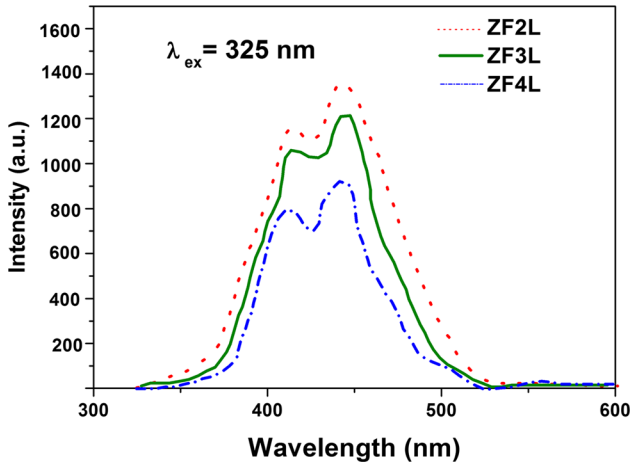

Fig. 7. PL EM of Zn-Fe LDH with different molar ratios.

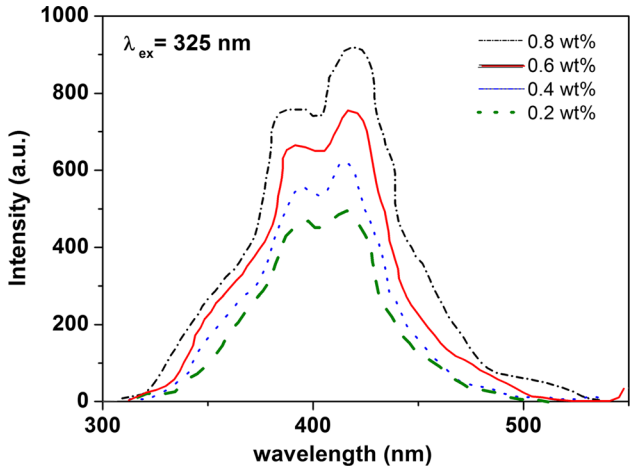

Fig. 8. PL EM spectra of Zn-Fe LDH colloids.

may be due to an increase in the crystallite size of Zn-Fe LDH with an increase in molar ratio; it leads to a decrease in surface charge density which is an important parameter for PL generation. Thus

decrease in surface charge density in ZF3 and ZF4 decreases PL intensities of ZF3L and ZF4L.

Figure 8 represents emission spectra of colloids at different wt.% of Zn-Fe LDH excited at 325 nm. It is interesting to observe an increase in PL intensity with an increase in LDH concentration, because increased concentration increases exfoliated nanosheets resulting in more traps or surface defects, which contribute to increased electron–hole recombination. The same shape of the emission spectra suggests the same origin of the PL effect in all colloids.

CONCLUSION

Zn-Fe LDHs with Zn^{2+}/Fe^{3+} molar ratios 2, 3 and 4 were successfully synthesized at constant pH 10 by a simple coprecipitation method at room temperature. XRD confirmed the crystallinity of Zn-Fe LDH. EDX showed the presence of Zn and Fe elements without any impurities. The average particle size calculated by using TEM micrographs was found to be 5–6 nm. Hexagonal nanosheets were also observed from TEM micrographs. These Zn-Fe LDHs were used to study the photoluminescence of their colloids with the organic solvent formamide. Results reveal that the PL property of Zn-Fe LDH depends on the Zn^{2+}/Fe^{3} molar ratio and concentration in formamide. The study showed different PL phenomenon in powdered Zn-Fe LDH and its colloids due to increased molecular interaction after delamination in formamide. An increase in PL emission intensities with a decrease in molar ratio and an increased concentration of LDH in corresponding colloids are due to increased surface charge density and surface defects, respectively. These results help us to understand optical properties, mainly photoluminescence, of pristine LDH and colloids of LDH. This may become an important contribution to applications that take advantage of LDH colloid's *luminescent* properties, such as bioimaging, solid-state lighting, and luminescent solar concentrators.

REFERENCES

1. J.S. Valente, F. Tzompantzi, J. Prince, G.H. Jose, and C.R. Gomez, *Appl. Catal. B: Environ.* 90, 330 (2009).
2. E. Dvininova, M. Ignata, P. Barvinschib, M.A. Smithersc, and E. Popovicia, *J. Hazard. Mater.* 177, 150 (2010).
3. Z.M. Ni, S.J.L. Xia, F.F. Wang, and G.P. Xing, *J. Colloid Interface Sci.* 316, 284 (2007).
4. C. Nethravathi, J.T. Rajamathi, N. Ravishankar, C. Shivakumara, and M. Rajamathi, *Langmuir* 24, 8240 (2008).
5. Y. Zhao, M. Wei, L. Jun, Z.L. Wang, and X. Duan, *ACS Nano* 3, 4009 (2009).
6. S.J. Palmer and R.L. Frost, *Ind. Eng. Chem. Res.* 49, 8969 (2010).
7. V. Prevot, N. Caperaa, C. Taviot-Gueho, and C. Forano, *Cryst. Growth Des.* 9, 3646 (2009).
8. B. Zümreoglu-Karan and A. Ay, *Chem. Pap.* 66, 1 (2012).
9. J.-H. Choy, J.-M. Oh, M. Park, K.-M. Sohn, and J.-W. Kim, *Adv. Mater.* 16, 1181 (2004).
10. L. Mohapatra and K. Parida, *J. Mater. Chem. A* 4, 10744 (2016).
11. F. Li and X. Duan, *Layered Double Hydroxides*, ed. X. Duan and D.G. Evans (Berlin: Springer, 2006), p. 193.
12. C. Del Hoyo, *Appl. Clay Sci.* (2007). https://doi.org/10.1016/j.clay.2006.06.010.
13. C. Aguzzi, P. Cerezo, C. Viseras, and C. Caramella, *Appl. Clay Sci.* 36, 22–36 (2007).
14. M.R. Berber, I.H. Hafez, K. Minagawa, T. Mori, and M. Tanaka, *Advances in Nanocomposite Technology*, ed. A.A. Hashim (InTech: Rijeka, 2011), p. 335.
15. P. Nalawade, B. Aware, V.J. Kadam, and R.S. Hirlekar, *J. Sci. Ind. Res.* 68, 267 (2009).
16. J.-H. Choy, S.-J. Choi, O. Jae-Min, and T. Park, *Appl. Clay Sci.* 36, 122 (2007).
17. S. Aisawa, N. Higashiyama, S. Takahashi, H. Hirahara, D. Ikematsu, H. Kondo, H. Nakayama, and E. Narita, *Appl. Clay Sci.* 35, 146 (2007).
18. S. Aisawa, H. Kudo, T. Hoshi, S. Takahashi, H. Hirahara, Y. Umetsu, and E. Narita, *J. Solid State Chem.* 177, 3987 (2004).
19. J.-C. Dupin, H. Martinez, C. Guimon, E. Dumitriu, and I. Fechete, *Appl. Clay Sci.* 27, 95 (2004).
20. E.M. Seftel, E. Dvininov, D. Lutic, E. Popovici, and C. Ciocoiu, *J. Optoelectron. Adv. Mater.* 7, 2869 (2005).
21. R.P. Wijitwongwan, S.G. Intasa-ard, and M. Ogawa, *Chem. Eng.* 3, 68 (2019).
22. P.S. Braterman, Z.P. Xu, and F. Yarberry, *In Handbook of Layered Materials*, ed. S.M. Auerbach, K.A. Carrado, and P.K. Dutta (New York: Marcel Decker Inc., 2004), p. 374.
23. E.L. Crepaldi, P.C. Pavan, and J.B. Valim, *J. Braz. Chem. Soc.* 11, 64 (2000).
24. K.M. Parida and L. Mohapatra, *Chem. Eng. J.* 179, 131 (2012).
25. C.R. Gordijo, V.R.L. Constantino, and D. de Oliveira Silva, *J. Solid State Chem.* 180, 1967 (2007).
26. F. Cavani, F. Trifiro, and A. Vaccari, *Catal. Today* 11, 173 (1991).
27. M.S. Gasser, *Colloids Surf. B: Biointerfaces* 73, 103 (2009).
28. N. Baliarsingh, L. Mohapatra, and K. Parida, *J. Mater. Chem. A* 1, 4236 (2013).
29. N. Baliarsingh, K.M. Parida, and G.C. Pradhan, *Ind. Eng. Chem. Res.* 53, 3834 (2014).
30. Y.C. Kang, H.S. Roh, D.J. Seo, and S.B. Park, *J. Mater. Sci. Lett.* 19, 1225 (2000).
31. Huang-Yu Chen, H.-L. Lai, R.-Y. Yang, and S.-J. Chang, *J. Mater. Sci.: Mater. Electron.* 27, 2963 (2016).
32. V. Choudhary, R. Jha, and P.A. Choudhary, *J. Chem. Sci.* 117, 635 (2005).
33. Z. Liu, R. Ma, M. Osada, N. Iyi, Y. Ebina, K. Takada, and T. Sasaki, *J. Am. Chem. Soc.* 128, 4872 (2006).
34. K. Okamoto, T. Sasaki, T. Fujita, and N. Iyi, *J. Mater. Chem.* 16, 1608 (2006).
35. F. Leroux and C. Taviot-Guého, *J. Mater. Chem.* 15, 3628 (2005).
36. W. Chen, L. Feng, and Q. Baojun, *Chem. Mater.* 16, 368 (2004).
37. L. Qiu and Q. Baojun, *J. Colloid Interface Sci.* 301, 347 (2006).
38. B.R. Venugopal, N. Ravishankar, C.R. Perrey, C. Shivakumara, and M. Rajamathi, *J. Phys. Chem. B* 110, 772 (2006).
39. L. Li, R. Ma, N. Iyi, Y. Ebina, K. Takada, and T. Sasaki, *Chem. Commun.* 29, 3125 (2006).
40. R. Ma, Z. Liu, L. Li, N. Iyi, and T. Sasaki, *J. Mater. Chem.* 16, 3809 (2006).
41. B. Li, J. He, D.G. Evans, and X. Duan, *J. Phys. Chem. Solids* 67, 1067 (2006).
42. H. Zhang, R. Qi, D.G. Evans, and X. Duan, *J. Solid State Chem.* 177, 772 (2004).
43. G. Fan, F. Li, D.G. Evans, and X. Duan, *Chem. Soc. Rev.* 43, 7040 (2014).
44. Z. Wang, F. Liu, and L. Chao, *Biosens. Bioelectron.* 60, 237 (2014).
45. E. Rauwel, A. Galeckas, P. Rauwel, and H. Fjellvåg, *Adv. Func. Mater.* 22, 1174 (2012).

46. Y. Zhao, J.-G. Li, M. Guo, and X. Yang, *J. Mater. Chem. C* 1, 3584 (2013).
47. X. Gao, X. Li, and Yu Weidong, *J. Phys. Chem. B* 109, 1155 (2005).
48. R.R. Piticescu, R.M. Piticescu, and C.J. Monty, *J. Eur. Ceram. Soc.* 26, 2979 (2006).
49. H.-M. Xiong, X. Yang, Q.-G. Ren, and Y.-Y. Xia, *J. Am. Chem. Soc.* 130, 7522 (2008).